New composite films based on MoO_{3-x} nanowires aligned in a liquid single crystal elastomer matrix

Valentina Domenici · Marjetka Conradi ·
Maja Remškar · Marko Viršek · Blaž Zupančič ·
Aleš Mrzel · Martin Chambers · Boštjan Zalar

Abstract In this study, we report the preparation, structure characterization, and application of new MoO_{3-x} nanowires, promising candidates for lithium intercalation, hydrogen sensing, and smart windows due to their photochromic property. These nanowires are a mixture of MoO_3 and conductive Mo_5O_{14} phase and have been used to prepare composite films based on liquid single crystal elastomers (LSCE). The structure, morphology, and thermomechanic behavior of these films are discussed. In particular, we show that the particular combination of molybdenum-based nanowires and LSCEs allows for doping of liquid single crystal elastomers, preserving the pristine mechanical and optical properties of the host matrix.

V. Domenici (✉)
Dipartimento di Chimica e Chimica Industriale,
Università di Pisa, Via Risorgimento 35, 56126 Pisa, Italy
e-mail: valentin@dcci.unipi.it

M. Conradi
Institute of Metals and Technology, Lepi pot 11,
1000 Ljubljana, Slovenia

M. Remškar · M. Viršek · B. Zupančič · A. Mrzel ·
M. Chambers · B. Zalar
J. Stefan Institute, Jamova 39, 1000 Ljubljana, Slovenia

M. Remškar
Centre of Excellence NAMASTE, Jamova 39,
1000 Ljubljana, Slovenia

M. Remškar
Centre of Excellence POLIMAT, Hajdrihova 19,
1000 Ljubljana, Slovenia

Introduction

The research in molybdenum oxides and their derivatives has been receiving significant attention especially with respect to applications in catalysis and as electrochemical devices [1–4]. The fabrication of molybdenum oxide material in nanostructured form and with anisotropic morphology appears to be a particularly attractive goal. Several preparation strategies to produce molybdenum oxide in the form of nanorods [5, 6], nanowires [7–9], and nanocrystals [10–13] are known, with stoichiometry MoO_3 or MoO_2, whereas little is known about a new kind of nanowires having a not standard stoichiometry, such as Mo_5O_{14} crystalline phase. On the other hand, Liquid Single Crystal Elastomers (LSCEs) represent a hot topic in Soft Matter since they belong to the sub-class of smart materials with "shape memory" properties, due to their ability to "memorize" the macroscopic shape [14] under specific conditions. Inserting nanoparticles into a liquid crystalline elastomeric matrix is very promising due to potential novel properties, like an ability to modify the shape by external electric and magnetic fields, and exploitation of temperature-controlled geometrical changes, unlike in usual LCE systems [15]. There are several examples in the literature [16–18] in which the interaction between nanoparticles, such as silica-based or carbon nanomaterials, and non-mesogenic polymeric matrices gives rise to an enhancement of intrinsic elastic and mechanical properties of the polymer [19–21]. The combination between the particular physical properties, such as conductivity or ferroelectricity of the nanoparticles and the thermo-elasticity and reversible thermo-mechanical response characteristic for LSCEs [22–24] leads to a few examples of composite materials retaining the shape-memory ability of LSCE systems [25–28]. Conductive composite systems have been recently

created by reprocessing standard liquid single crystal elastomer (LSCE) films with carbon nanoparticles through a gel-swelling technique [29–31]. These new materials, consisting of a conductive layer at the surface of the LSCE films, exhibit interesting properties, such as the piezoresistivity [32].

In this study, we are reporting on a successful preparation of composite films having a liquid crystalline elastomer matrix and Mo-oxides nanowires as inorganic conductive component. A special kind of nanowires with non-standard stoichiometry, composed of a mixture of MoO_3 and Mo_5O_{14} crystalline phases, was prepared and characterized. Basic features of the morphology and thermo-mechanic behavior of these new composites will be discussed. Field Emission (FE) Scanning Electron Microscopy (SEM), recently used also to study a star-shape type of MoO_2 nanomaterials [13], and Atomic Force Microscopy (AFM) techniques were applied to the study of the new composite films to clarify the morphology and averaged dimensions of the nanowires used in the preparation of the new composite materials as well as their relative orientation in the LSCE matrix.

Experimental

Synthesis of MoO_{3-x} nanowires

The mixture of MoO_3 and Mo_5O_{14} nanowires was synthesized using $Mo_6S_2I_8$ nanowires as a starting material [33]. The $Mo_6S_2I_8$ nanowires were placed into a quartz tube, closed at one side, with dimensions of 1000 mm in length and 32 mm in diameter. The material was annealed in air in one-zone oven at 603 K for 2 h. A trap, cooled with water, was placed at the open side of the quartz tube. The trap served for collecting the iodine released and simultaneously enabled the access of the air to the material in the boat that enables a growth of MoO_{3-x} phase. The blue colored nanowires of molybdenum sub-oxides have grown, retaining the basic shape and a toughness of the starting nanowires.

Preparation of liquid crystalline elastomer composites

The new composite films based on LSCE matrix were prepared according to the following procedure. A homogeneous dispersion of MoO_{3-x} nanowires, synthesized as described in "Synthesis of MoO_{3-x} nanowires," in toluene was prepared by ultrasonification for about 30 min. A concentration of about 1% in weight of nanowires was used. One milliliter of such dispersion was added to 1 mL of pre-polymerization toluene-solution, whose components are: the polymeric chain (1) hydroxymethyl-polysiloxane

(1 mmol), the mesogen (2) 4-methoxyphenyl 4-(but-3-en-1-yloxy) benzoate (0.85 mmol) and the crosslinker (3) 1,4-bis(undec-10-en-1-yloxy) benzene (0.075 mmol). A sketch of the molecular structure of the main components of the LSCE is reported in Scheme 1. Syntheses of components (2) and (3) were performed as described in [34]. The chemical structure and purity of all these compounds were checked by means of ^1H and ^{13}C NMR in solution. A commercial platinum catalyst (COD from Wacker Chemie) was added to the final mixture. To produce monodomain LSCE films, we used the well-known two-step crosslinking technique, pioneered by Kupfer and Finkelmann [35]. The prepared mixture was inserted into a circular reactor inside a modified centrifuge. A rate of 4500 rpm and an average temperature of 343 K were set for an hour to prepare a partially crosslinked film network, swollen by the solvent. The second step of crosslinking reaction consists of slowly removing the solvent under progressive increasing loads at room temperature, followed by 3 days of drying at 343 K under constant load.

Following this procedure, we have obtained several composite films of similar thickness and shape, with a
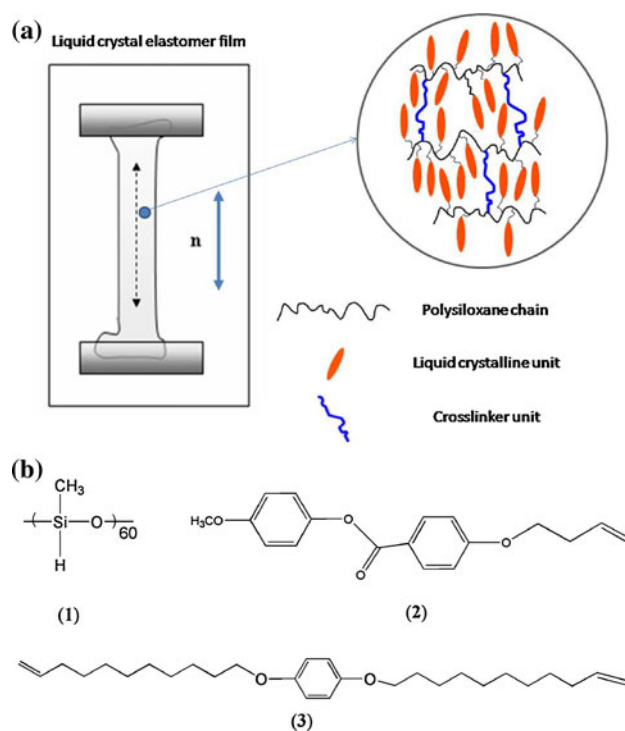
Scheme 1 a Liquid single crystal elastomer film: the director, **n**, along the stress direction, is shown with a double *arrow*. The *inset* on the *right* shows an illustrative sketch of the composition of the liquid crystalline elastomeric matrix at the nanoscale and the main components: polysiloxane chains, mesogenic units and crosslinker moieties. **b** Chemical formula of the polysiloxane chain (1), mesogenic unit (2) and crosslinker (3) used in the preparation of the investigated samples

uniaxial orientation of the local directors, which results in monodomain stripes. A standard LSCE stripe, without nanowires, was also prepared by following exactly the same procedure (without adding the nanowires dispersion to the pre-polymerization mixture) with the same chemical composition [36], namely $n = 85\%$ of (2) and $m = 7.5\%$ of (3). Polydomain samples, obtained without mechanically loading the gel-films during the second crosslinking step, were also prepared. In all cases, the completeness of the crosslinking reaction was verified by means of Fourier Transform Infrared (FTIR) spectroscopy, by looking at the disappearance of the typical Si–H signal ($\tilde{\nu} \approx 2200\,\mathrm{cm}^{-1}$). All the prepared films were then swollen in toluene and dried in the oven at about 320 K. This procedure was repeated several times, depending on the sample, to ensure that no unreacted mesogens or crosslinkers were still present in the network. The absence of unreacted compounds was also checked by ^{1}H NMR and FTIR.

Characterization

MoO_{3-x} nanowires were studied using electron transmission microscopy 200 keV Jeol 2010F, scanning electron microscopy (FE-SEM, Supra 35 VP, Carl Zeiss), and X-ray diffraction (Siemens D-5000). The chemical composition of the basic components (2 and 3) of the LSCE composites was investigated by means of NMR (Varian VXR 300 spectrometer working at 300 MHz (^{1}H) and 75 MHz (^{13}C) using TMS as internal standard and $CDCl_3$ as solvent). Infrared spectra were recorded on a Perkin-Elmer FTIR 1725x spectrometer. The mesophase behavior of the new composite materials has been investigated by Perkin-Elmer DSC 7 calorimeter (DSC) at the second heating and cooling cycles with a rate of 10 K/min. Thermo-mechanic measurements have been performed on a home-built set up, constituted of a temperature-controlled glass tube, in which the composite film was suspended, and a computer-controlled digital camera. The variations of the film length were recorded as a function of temperature at different heating/cooling rates. Atomic force microscopy (AFM, Veeco Instruments, Multi Mode AFM, Nanoscope V) in tapping mode has been applied to image the soft surface of composite films and organization of inserted MoO_{3-x} nanowires. This method enables to obtain both topographical data of the sample and phase images with enhanced contrast, where the phase angle that measures the phase lag of the cantilever oscillation relative to the excitation force contains the information about the interaction between the tip and the sample. To probe the surface, we used TESPA Veeco probes with a hard tip of elastic constant 20–80 N/m and frequency between 310 and 337 kHz.

Results and discussion

Structure and morphology of the MoO_{3-x} nanowires

The MoO_{3-x} nanowires have diameters up to 500 nm and length of several millimeters as determined by means of TEM and SEM techniques (Fig. 1a, b). TEM images (Fig. 1c) show that triangular thin flakes protrude in radial direction with respect to the nanowire axis. These protrusions enlarge the reactive surface of the nanowires and evidence that the temperature during the transformation process was sufficiently high for translocation of part of molybdenum by diffusion. The nanowires are partially polycrystalline, although the electron diffraction resembles a single crystal pattern. This can be explained in terms of strong texturing of the crystallites. The particular Mo_5O_{14} phase was determined on a single nanowire based on transmission electron diffraction patterns (Fig. 1d), while the X-ray spectrum is not distinguishable from the MoO_3 one (Fig. 2). Moreover, these nanowires are found to be electrically conductive and highly porous, with promising applications in lithium intercalation, catalysis, field emission devices, and as strengthening fibers.

### Thermal and thermomechanic behavior of LSCE-based composites

Differential scanning calorimetry of the new LSCE-based composites confirmed the typical thermal behavior of polysiloxane-based LSCEs: all samples have a nematic phase stable in a large temperature range (from ~ 269 to ~ 347 K). The presence of a low concentration of MoO_{3-x} nanowires (~ 1 wt%) is responsible of a slight shift of the transition temperatures of a few degrees (both isotropic-nematic and nematic-glass phase transitions) with respect to the standard LSCE stripes prepared with the same procedure and chemical composition [15, 36]. Significantly, the presence of nanowires does not alter the thermal properties of the LSCE matrix and the thermal behavior is reproducible after several heating–cooling cycles. The mesophase transitions of the prepared standard LSCE and LSCE-based composite stripes, as determined by DSC, are reported in Table 1.

The most important feature of the LSCE-based composite films is the homogeneous distribution of the local nematic director, **n**, along the stretching direction. The preparation procedure, known as two-step crosslinking technique pioneered by Kupfer and Finkelmann [35], ensured the homogeneity of the monodomain films, as it can be seen from the transparency of the films shown in Fig. 3a. The obtained composite films have similar thickness ($\sim 150\,\mu m$) and a rectangular shape ($\sim 2/3$ cm in
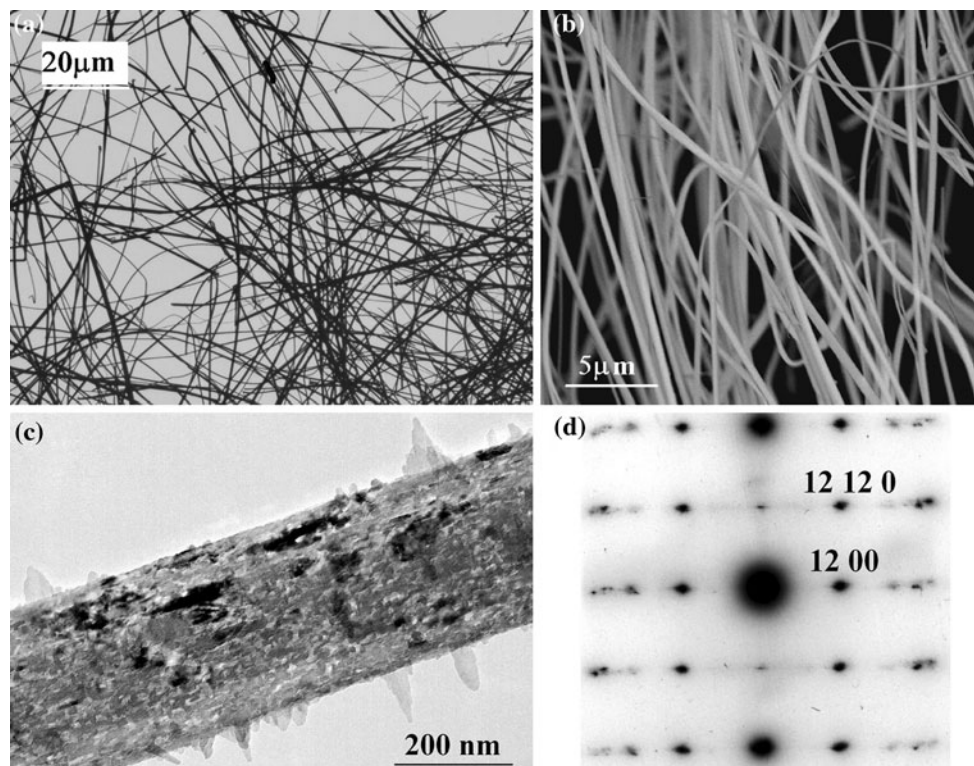
Fig. 1 The MoO_{3-x} nanowires. **a** A typical TEM image of millimeter-long nanowires; **b** a SEM image revealing sufficient electrical conductivity of 10 keV observation without a special sample preparation; **c** a TEM image of a single nanowires with polycrystalline structure and tip-shaped protrusions on the surface; **d** A transmission electron diffraction on a single nanowire revealing a single crystal pattern and assigned in accordance with JCPDS No. 074-1415
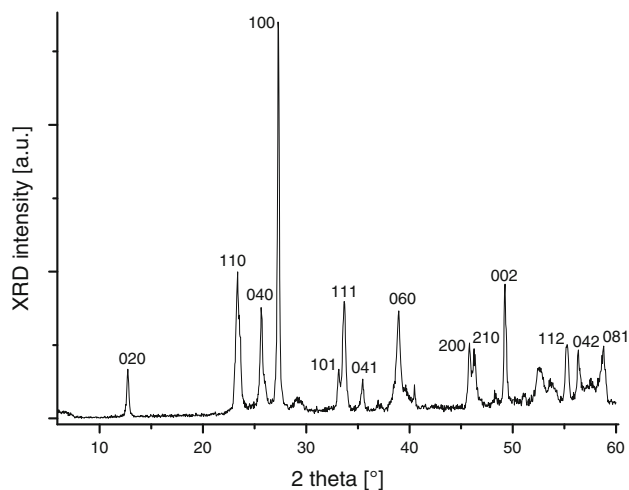
Fig. 2 XRD spectrum of molybdenum oxide nanowires synthesised by oxidation of the $Mo_6S_2I_8$ precursor nanowires at 603 K. In the spectrum the MoO_3 phase can be identified with the most intensive peaks assigned to reflections according to the orthorhombic primitive lattice [JCPDS 05-0508]

length and ~ 5 mm in width), with a uniaxial orientation of the local directors, **n**, as shown in Scheme 1 and Fig. 3a.

Figure 3b reveals the trend of the mechanical elongation ratio ($=L/L_0$) of a LSCE-based composite stripe with

Table 1 Temperatures, T (K), enthalpies, ΔH (J/g), and specific heat, ΔC_p (J/gK), of the phase transitions of the investigated samples

Sample	Glass	ΔC_p	T	Nematic	ΔH	T	Isotropic
Standard LSCE	●	0.33	269.2	●	2.98	346.8	●
LSCE-based composite	●	0.25	265.8	●	2.76	347.5	●

The bullets indicate the existence of the mesophase

temperature. The reproducibility of this trend after many sweeps is an indication of the quality of the composite with no degradation effect produced by the added nanowires [37]. The temperature trend of the ratio L/L_0 confirms that the LSCE-based composite films have a homogeneous orientation of the nematic director (Fig. 3a). The elongation (L/L_0) of the composite film under minimal stress (~ 100 mg) is about 58% at room temperature with respect to its length in the isotropic phase (L_0). This value is comparable with the elongation of the standard LSCEs [36], which is about 68%, and it proves that the peculiar LSCE properties are retained in the nanowires-LSCE composite films investigated in this study.

Fig. 3 a Two monodomain stripes of the LSCE-based composites containing the MoO_{3-x} nanowires; the director **n** is displayed. **b** Thermomechanic measurements of the composite LSCE-based monodomain films under minimal stress (~ 100 mg) obtained in the process of cooling the sample from the isotropic phase down to room temperature
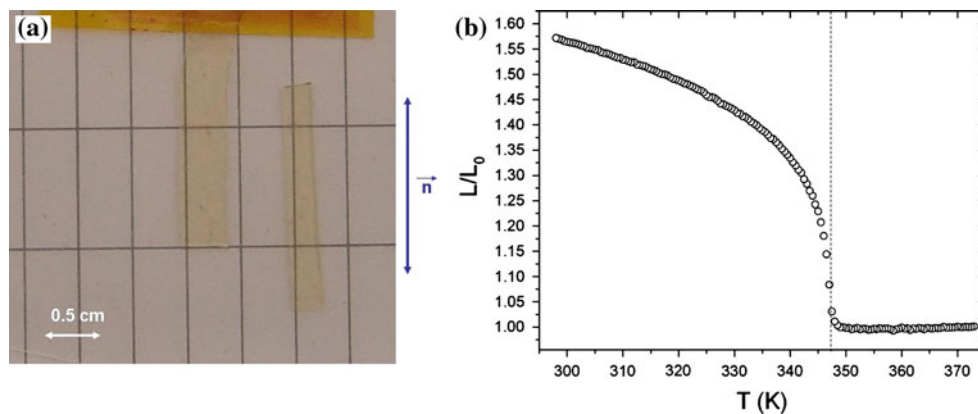
Morphology and nanowire distribution in the LSCE-based composites

The morphology and in particular the distribution of the nanowires in the LSCE matrix were investigated by means of optical microscopy, field emission SEM, and AFM microscopy. Optical microscope in transmission mode with crossed-polarisers reveals the MoO_{3-x} nanowires as white, while LSCE matrix is black. The distribution of nanowires and their orientation with respect to the local nematic directors is shown in Fig. 4.

The homogeneity of the LSCE nanocomposite cross section (Fig. 4a) is demonstrated via the uniformity of light extinction when viewed with polarized light; the film thickness is around 0.3 mm. Most of the MoO_{3-x} nanowires are distributed on the top surface of the composite films. This is probably due to the fact that, during the first cross-linking step, the Mo-oxides nanowires tend to separate from the rest of pre-polymerization components because of the different relative weight [15, 36]. In fact, Mo-oxides nanowires are deposited at the inner side of the swollen film inside the centrifuge rotor. Moreover, the white lines seen in Fig. 4b indicate a uniform alignment of the nanowires along the director **n**, thus indicating that the adopted procedure allowed us to induce a preferred alignment of the nanomaterials into the top surface of the LSCE matrix.
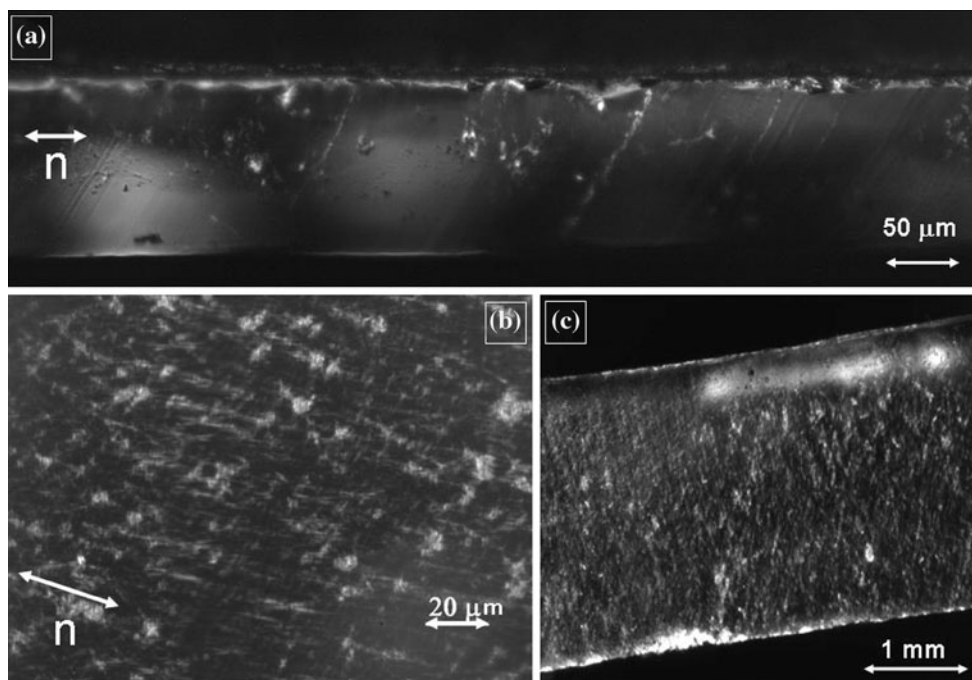
Fig. 4 Optical images of the LSCE-based composite film: **a** cross section, **b, c** the top surface MoO_{3-x} nanowires are shown as white stripes in contrast with the black matrix. The alignment direction of the local director **n** is shown as well

Fig. 5 AFM topography image (*left*) and phase image (*right*) of composite film surface showing MoO_{3-x} nanowires dipping into the polymer matrix
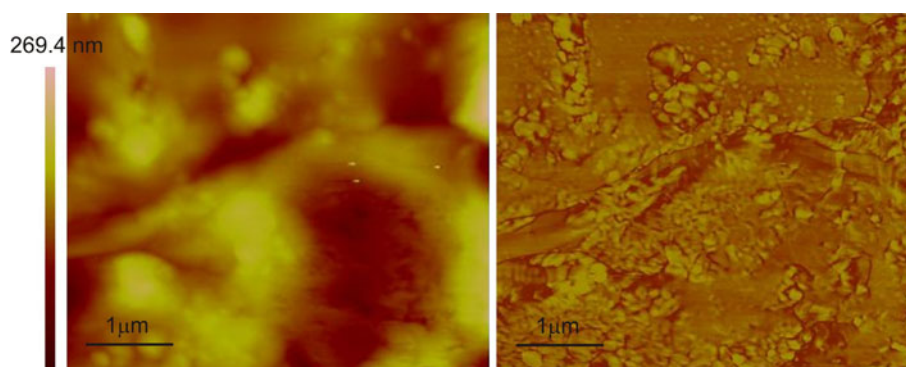
Topography and phase imaging modes were used to probe the surface of LSCE-based composite films and organization of MoO_{3-x} nanowires. As shown in Fig. 5, the surface of these composites is inhomogeneous with roughness of the order of tenths of nanometers. Although the nanowires are positioned close to the surface of LSCE, they are well embedded into the surface layer of the polymer matrix.

In addition, on some parts of the new composite films, we observe characteristic surface deformations (Fig. 6) which appear due to minimization of free energy. In elastomeric systems, chemically similar to LSCEs [38], these deformations have been described by Euler strut instabilities, typical for a pair of adjacent elastic media of a different Young modulus. Specifically, since the surface layer has different elastic moduli from the bulk, it is spontaneously deformed when a compressive force is applied in the direction along the surface. This phenomenon results in a sinusoidal modulation of the surface height, with a well-defined periodicity [30, 39]. The mechanism of deformation, however, strongly depends on the ratio of elastic contributions of the surface and bulk material as well as the layer thickness. According to the available data for similar LSCE-composites [31, 32, 36, 39], the ratio between elastic Young modulus at the surface and in the LSCE bulk well justifies the observed wrinkle wavelength λ of few microns [40].

Moreover, the different temperature dependences of the surface and bulk Young modulus [41] does not exclude the possibility to tune the wrinkle wavelength as a function of the temperature, opening to new applications.
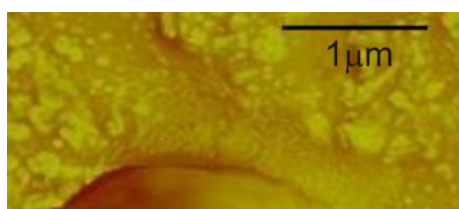
Fig. 6 Surface of the composite film with characteristic undulations

Conclusions

The composite films described in this study contain conductive MoO_{3-x} nanowires as inorganic component and LSCE matrix as organic one. The properties of these composite films show several similarities with those of the conductive LSCE-nanocarbon systems prepared by Chambers et al. [29–32, 39], made of a conductive thin layer of carbon nanoparticles on the top surface of a LSCE matrix. However, the peculiarity of these films is that the Mo-oxides nanowires are homogeneously distributed on the top surface of the film [38] with a homogeneous alignment parallel to the local nematic directors, **n**. The particular distribution of the nanowires reflects the influence of the first step of crosslinking inside the centrifuge rotor, which is responsible of the deposition of the MoO_{3-x} nanowires on one side of the film. On the other hand, the parallel alignment of the nanowires with respect to the nematic director is a direct consequence of the second step of crosslinking reaction and indicates a coupling between the local mesogen orientational order and the spatial distribution of nanowires. A similar behavior has been observed on $PbTiO_3$ nanoparticles-doped LSCE [15, 28]; in that case, the ferroelectric nanoparticles (of quasi-spherical shape) were distributed in stripes perpendicularly to the director, **n**. These works clearly show that the adopted preparation procedure is crucial to get aligned nanomaterials within the LSCE matrix.

In the case reported in this article, the peculiar alignment of the MoO_{3-x} nanowires is most probably due to a coupling between the dipoles of the LC mesogens and that of the nanowires.

Compared with other nanoparticle-elastomer composite materials [15, 28–32, 42–44], the conductivity of the MoO_{3-x} nanowires is expected to give a more immediate application of these films as conductive actuators.

References

1. Chen W, Xu Q, Hu YS, Mai LQ, Zhu QY (2002) J Mater Chem 12:1926
2. Dobley A, Ngala K, Yang S, Zavalij PY, Whittingham MS (2001) Chem Mater 13:4382
3. Tian LP, Li WSh, Li H (2000) Mod Chem Ind 20:19
4. Chandrappa GT, Steunou N, Cassaignon S, Bauvais C, Bisas PK, Livage J (2003) J Sol–Gel Sci Technol 26:593
5. Wu XC, Tao YR, Dong L, Hong JM (2004) J Mater Chem 14:901
6. Chen W, Mai L, Qi Y, Dai Y (2006) J Phys Chem Solids 67:896
7. Li Q, Newberg JT, Walter EC, Hemminger JC, Penner RM (2004) Nano Lett 4:277
8. Zhou J, Xu N, Deng S, Chen J, She J, Wang Z (2003) Adv Mater 15:1835
9. Wang T, Zhang Y, Wang W, Li G, Ma X, Li X, Zhang Z, Qian Y (2006) J Cryst Growth 260:92
10. Merchan-Merchan W, Saveliev AV, Desai M (2009) Nanotechnology 20:475601
11. Chernova NA, Roppolo M, Dillon AC, Whittingham MS (2009) J Mater Chem 19:2526
12. Lee SH, Deshpande R, Parilla P, Jones K, To B, Bobby M, Harv D (2007) American Physical Society March Meeting, March 5–9, 2007, abstract #V42.009
13. Khademi A, Azimirad R, Zavarian AA, Moshfegh AZ (2009) J Phys Chem C 113:19298
14. Warner M, Terentjev EM (2003) Liquid crystal elastomers. Oxford University Press, Oxford
15. Domenici V, Zupancic B, Laguta VV, Belous AG, V'yunov OI, Remskar M, Zalar B (2010) J Phys Chem C 114:10782
16. Vast L, Carpentier L, Lallemand F, Colomer JF, Van Tendeloo G, Fonseca A, Nagy JB, Mekhalif Z, Delhalle J (2009) J Mater Sci 44:3476. doi:10.1007/s10853-009-3464-1
17. El Fray M, Boccaccini AR (2005) Mater Lett 59:2300
18. Bandyopadhyaya R, Rong WZ, Fredlander SK (2004) Chem Mater 16:3147
19. Dasaroyong K, Yeonseok K, Kyungwho C, Jaime C, Choongho Y (2010) ACS Nano 4:513
20. Rossi GB, Beaucage G, Dang TD, Vaia RA (2002) Nano Lett 2:319
21. Babski K, Boczkowska A, Kurzydlowski KJ (2009) J Mater Sci 44:1456. doi:10.1007/s10853-008-3036-9
22. Ahir SV, Terentjev EM (2005) Nat Mater 4:491
23. Courty S, Mine J, Tajbakhsh AR, Terentjev EM (2003) Europhys Lett 64:654
24. Domenici V, Ambrozic G, Copic M, Lebar A, Drevensek-Olenik I, Umek P, Zalar B, Zupancic B, Zigon M (2009) Polymer 50:4837
25. Huang YY, Ahir SV, Terentjev EM (2006) Phys Rev B 73:125422
26. Shenoy DK, Thomsen D L III, Srinivasan A, Keller P, Ratna BR (2002) Sens Actuators A 96:184
27. Kim KJ, Shahinpoor M (2002) Polymer 43:797
28. Domenici V, Zupancic B, Remskar M, Laguta VV, Veracini CA, Zalar B (2009) In: Vincenzini P, BarCohen Y, Carpi F (eds) Artificial muscles actuators using electroactive polymers. Advances in science and technology book series, vol 61, p 34. Trans Tech Publications Ltd, Stafa-Zurich, Switzerland
29. Chambers M, Zalar B, Remskar M, Finkelmann H, Zumer S (2006) Appl Phys Lett 89:243116
30. Chambers M, Zalar B, Remskar M, Kovac J, Finkelmann H, Zumer S (2007) Nanotechnology 18:415706
31. Chambers M, Zalar B, Remškar M, Finkelmann H, Zumer S (2008) Nanotechnology 19:155501
32. Chambers M, Finkelmann H, Remskar M, Sánchez-Ferrer A, Zalar B, Zumer S (2009) J Mater Chem 11:1524
33. Remskar M, Mrzel A, Virsek M, Jesih A (2007) Adv Mater 19:4276
34. Sánchez-Ferrer A (2006) Photo-active liquid crystalline elastomers, Ph. D. Thesis, Facultat de Quimiques, Departament de Quimica Organica, Barcelona
35. Kupfer J, Finkelmann H (1991) Makromol Chem Rapid Commun 12:717
36. Domenici V, Zalar B (2010) Phase Transit 83:1014
37. Domenici V, Conradi M, Remskar M, Mrzel A, Zalar B (2011) In: Vincenzini M, Ferrari M (eds) Advances in science and technology, vol 71, pp 40–44
38. Bowden N, Brittain S, Evans AG, Hutchinson JW, Whiteside GM (1998) Nature 393:146
39. M. Chambers (2007) Jozef Stefan Institute, Ljubljana, PhD Thesis
40. Cerda E, Mahadevan L (2003) Phys Rev Lett 90:074302
41. Finkelmann H, Greve A, Warner M (2001) Eur Phys J E 5:281
42. Coffey AB, O'Bradaigh CM, Young RJ (2007) J Mater Sci 42:8053. doi:10.1007/s10853-007-1680-0
43. Sánchez-Ferrer A, Reufer M, Mezzenga R, Schurtenberger P, Dietsch H (2010) Nanotechnology 21:185603/1
44. Finkelmann H, Shahipoor M (2002) In: Bar-Cohen Y (ed) Smart structures and materials, electroactive polymer actuators and devices (EAPAD), vol 4695, pp 459–464